A Computational Methodology to Select the Optimal Material Combination in Laminated Composite Pressure Vessels

PAVEL Y. TABAKOV
Durban University of Technology
Department of Mechanical Engineering
P.O. Box 1334, Durban, 4000
SOUTH AFRICA
pashat@dut.ac.za

MARK WALKER
Durban University of Technology
Department of Mechanical Engineering
P.O. Box 1334, Durban, 4000
SOUTH AFRICA
walker@dut.ac.za

Abstract: A methodology to select the best material combination and optimally design laminated composite pressure vessels is described. The objective of the optimization is to maximize the critical internal pressure subject to cost constraints. Exact elasticity solutions are obtained using the stress function approach, where the stresses are determined taking into account the closed ends of the cylindrical shell. The approach used here allows us to analyze accurately multilayered pressure vessels with an arbitrary number of orthotropic layers of any thickness and a combination of different materials. The design optimization of the pressure vessel is accomplished using the Big Bang–Big Crunch algorithm,subject to the Tsai-Hill failure criterion.

Key–Words: Composites, pressure vessel, exact solution, optimal design, material selection.

1 Introduction

The increased use of laminated composite piping and pressure vessels in many engineering applications has led to a need for more accurate stress-strain analysis. Their resistance to corrosion along with high strength to weight ratios and relatively low densities compared to other traditional materials makes them indispensable in the chemical, petrochemical, marine and aerospace industries. The versatility of composite materials offers opportunities and the flexibility to tailor such structures according to needs. The tailoring is mostly achieved by maximizing the mechanical properties as a result of selecting the fiber angles of the layers optimally. Obviously, such design optimization comes at a cost. This has created a need for further progress in such classical areas of mechanics as the theory of anisotropic and non-homogeneous deformable solids, and the theory of optimization.

Despite a tremendous effort to uncover what others have done, it appears that no researchers have dealt with the selection of the best material combinations for the design optimization of pressure vessels. The usual constraints dealt with in design optimization are mass, cost and geometrical characteristics. In this paper a cost constraint is considered. Examples of procedures to select the best material combination and optimally design composite plates and cylindrical shells for minimum cost and mass are presented by Walker et al. [9, 10].

In this study, the optimal material combination in laminated pressure vessels is determined. The pressure vessels are optimized for maximum internal pressure subject to a maximum cost constraint. The problem considered is complicated and requires the use of a reliable optimization method. The present study implements a new approach using the Big Bang–Big Crunch (BB-BC) optimization method which was proposed by Erol and Eskin in 2006 [2] as a new evolutionary algorithm. The algorithm has proven to be exceptionally fast and efficient compared to genetic algorithms. This is especially true where the number of the design parameters is rather large and genetic algorithms become slow and inefficient [7].

Two types of pressure vessels have been used for the design optimization, – thin and moderately thick. Because of anisotropy and the presence of curvature in shell structures, obtaining exact three-dimensional elasticity solutions for laminated pressure vessels presents considerable complexity. Analytical solutions accounting for the three-dimensional nature of the stress-strain state in orthotropic cylinders have been developed by a number of researchers. The exact analytical analysis used in the present study was developed by Tabakov and Summers in [6]. The combination of accurate analysis and an efficient optimization algorithm has allowed we, the authors, to determine the results presented here used to demonstrate the methodology.

ISBN: 978-1-61804-146-3

2 Problem Description

2.1 Basic equations

The structure under consideration is a cylindrical shell of finite length made from an anisotropic material. The axis of anisotropy coincides with the axis of symmetry Oz of the cylinder and the stresses act on the planes normal to the generator and do not vary along the generator. Let $U,\ V$ and W be the functions which represent the displacement due to elastic deformation:

$$\begin{aligned} \frac{\partial U}{\partial r} &= \beta_{11}\sigma_r + \beta_{12}\sigma_\theta + \ldots + \beta_{16}\tau_{r\theta} \\ \frac{1}{r}\frac{\partial V}{\partial \theta} + \frac{U}{r} &= \beta_{12}\sigma_r + \beta_{22}\sigma_\theta + \ldots + \beta_{26}\tau_{r\theta} \\ \frac{1}{r}\frac{\partial W}{\partial \theta} &= \beta_{14}\sigma_r + \beta_{24}\sigma_\theta + \ldots + \beta_{46}\tau_{r\theta} \\ \frac{\partial W}{\partial r} &= \beta_{15}\sigma_r + \beta_{25}\sigma_\theta + \ldots + \beta_{56}\tau_{r\theta} \\ \frac{1}{r}\frac{\partial U}{\partial \theta} + \frac{\partial V}{\partial r} - \frac{V}{r} &= \beta_{16}\sigma_r + \beta_{26}\sigma_\theta + \ldots + \beta_{66}\tau_{r\theta} \end{aligned} \tag{1}$$

The distribution of the stresses will be identical in all cross sections and will depend only on the distance r from the axis. Therefore, the stresses can be expressed in terms of stress functions Φ and Ψas [4]

$$\sigma_r = \frac{1}{r}\frac{\partial \Phi}{\partial r} + \frac{1}{r^2}\frac{\partial^2 \Phi}{\partial \theta^2} + \overline{U}, \qquad \sigma_\theta = \frac{\partial^2 \Phi}{\partial r^2} + \overline{U}$$
$$\tau_{r\theta} = \frac{\partial^2}{\partial r \partial \theta}\left(\frac{\Phi}{r}\right),\ \tau_{rz} = \frac{1}{r}\frac{\partial \Psi}{\partial \theta},\ \tau_{\theta z} = -\frac{\partial \Psi}{\partial r} \tag{2}$$

where $\overline{U}$ is the potential of the body forces. The normal stress in the longitudinal direction can be given as

$$\sigma_z = -\frac{1}{\alpha_{33}}(\alpha_{13}\sigma_r + \alpha_{23}\sigma_\theta + \alpha_{34}\tau_{\theta z} + \alpha_{35}\tau_{rz} + a_{36}\tau_{r\theta}) \tag{3}$$

where α_{ij} are components of the compliance matrix. It should be noted that equation (3) is correct only for open ended cylinders or those without applied longitudinal forces, otherwise an additional constant needs to be added.

The approach formulated above may be used for the analysis of pressure vessels that are constructed of filament–wound layers with a fibre orientation of $(\pm\varphi^\circ)$. Due to asymmetrical loading and geometry, the distribution of the stresses will be identical in all cross sections and will depend only on the distance r from the axis. Therefore the stresses can be expressed in terms of stress functions proposed by Lekhnitskii [4] $\Phi_m = \Phi_m(r)$, $\Psi_m = \Psi_m(r)$ as

$$\sigma_r^{(m)} = \frac{1}{r}\frac{d\Phi_m}{dr};\ \ \sigma_\theta = \frac{d^2\Phi_m}{dr^2};\ \ \tau_{\theta z}^{(m)} = -\frac{d\Psi_m}{dr} \tag{4}$$

and longitudinal stress

$$\sigma_z^{(m)} = C - \frac{1}{\alpha_{33}^{(m)}}(\alpha_{13}^{(m)}\sigma_r^{(m)} + \alpha_{23}^{(m)}\sigma_\theta^{(m)} + \alpha_{34}^{(m)}\tau_{\theta z}^{(m)}) \tag{5}$$

Moreover, due to symmetry

$$\tau_{rz}^{(m)} = \tau_{r\theta}^{(m)} = 0 \tag{6}$$

In the above equations index m denotes the *m-th* layer and $m = 1, 2, \ldots, nl$ with nl denoting the total number of layers.

By eliminating U, V and W from the system of equations (1) by means of differentiation and taking into account the above assumptions the new system of differential equations takes the following form [4]:

$$\begin{aligned} & \beta_{22}^{(m)}\left(\frac{d^4\Phi_m}{dr^4} + \frac{2}{r}\frac{d^3\Phi_m}{dr^3}\right) \\ + \ & \beta_{11}^{(m)}\left(-\frac{1}{r^2}\frac{d^2\Phi_m}{dr^2} + \frac{1}{r^3}\frac{d\Phi_m}{dr}\right) \\ - \ & \beta_{24}^{(m)}\frac{d^3\Psi_m}{dr^3} + (\beta_{14}^{(m)} - 2\beta_{24}^{(m)})\frac{1}{r}\frac{d^2\Psi_m}{dr^2} = 0 \end{aligned} \tag{7}$$

$$\begin{aligned} - \ & \beta_{24}^{(m)}\frac{d^3\Phi_m}{dr^3} - (\beta_{14}^{(m)} - \beta_{24}^{(m)})\frac{1}{r}\frac{d^2\Phi_m}{dr^2} \\ + \ & \beta_{44}^{(m)}\left(\frac{d^2\Psi_m}{dr^2} + \frac{1}{r}\frac{d\Psi_m}{dr}\right) - \frac{1}{r}Ca_{34}^{(m)} = 0 \end{aligned} \tag{8}$$

where $\beta_{ij}^{(m)}$ are elastic constants given by

$$\beta_{ij}^{(m)} = \alpha_{ij}^{(m)} - \frac{\alpha_{i3}^{(m)}\alpha_{j3}^{(m)}}{\alpha_{33}^{(m)}}, \qquad i,j = 1,2,4 \tag{9}$$

2.2 Computation of Stresses

The boundary conditions on the internal $(r = a_0)$ and external $(r = a_{nl})$ surfaces are specified as

$$\sigma_r^{(1)}(a_0) = -p_0; \qquad \sigma_r^{(nl)}(a_{nl}) = -p_{nl} \tag{10}$$

where $a_0, \ldots, a_m, \ldots, a_{nl}$ are the radii measured from inside to outside. At the contact surfaces of adjacent layers we have the conditions

$$\sigma_r^{(m)} = \sigma_r^{(m+1)}, u_r^{(m)} = u_r^{(m+1)}, u_\theta^{(m)} = u_\theta^{(m+1)} \tag{11}$$

The equilibrium of forces on the end surfaces gives

$$2\pi\sum_{m=1}^{nl}\int_{a_{m-1}}^{a_m}\sigma_z^{(m)} r dr = \pi(p_0 - p_{nl})a_0^2 + F \tag{12}$$

where F is the applied axial force.

With regards to the condition (11) and taking into account the assumptions on physical and geometrical properties given above, the general solution of the system (8) has the following form [4]

$$\begin{aligned}
\Phi_m &= C\zeta_1^{(m)}\frac{r^2}{2} + \frac{C_1}{1+k_m}r^{1+k_m} + \frac{C_2}{1-k_m}r^{1-k_m} \\
\Psi_m &= Cr\left(\frac{\alpha_{34}^{(m)}}{\beta_{44}^{(m)}} + \zeta_1^{(m)}g_1^{(m)}\right) \qquad (13) \\
&+ C_1\frac{1}{k_m}g_k^{(m)}r^{k_m} - C_2\frac{1}{k_m}g_{-k}^{(m)}r^{-k_m}
\end{aligned}$$

where r is the radius, while $\zeta_1^{(m)},\ k_m,\ g_1^{(m)},\ g_k^{(m)}$ and $g_{-k}^{(m)}$ are β–dependent coefficients given by

$$\zeta_1^{(m)} = \frac{(\alpha_{13}^{(m)} - \alpha_{23}^{(m)})\beta_{44}^{(m)} - \alpha_{34}^{(m)}(\beta_{14}^{(m)} - \beta_{24}^{(m)})}{\beta_{22}^{(m)}\beta_{44}^{(m)} - \beta_{24}^{(m)2} - (\beta_{11}^{(m)}\beta_{44}^{(m)} - \beta_{14}^{(m)2})}$$

$$k_m = \sqrt{\frac{\beta_{11}^{(m)}\beta_{44}^{(m)} - \beta_{14}^{(m)2}}{\beta_{22}^{(m)}\beta_{44}^{(m)} - \beta_{24}^{(m)2}}},\quad g_1^{(m)} = \frac{\beta_{14}^{(m)} + \beta_{24}^{(m)}}{\beta_{44}^{(m)}}$$

$$g_k^{(m)} = \frac{\beta_{14}^{(m)} + k\beta_{24}^{(m)}}{\beta_{44}^{(m)}},\quad g_{-k} = \frac{\beta_{14}^{(m)} - k_m\beta_{24}^{(m)}}{\beta_{44}^{(m)}}$$

The stresses $\sigma_r^{(m)},\ \sigma_\theta^{(m)}$ and $\tau_{\theta z}^{(m)}$ can be calculated from equations (4), viz.

$$\begin{aligned}
\sigma_r^{(m)} &= C\zeta_1^{(m)} + C_1r^{k_m-1} + C_2r^{-k_m-1} \\
\sigma_\theta^{(m)} &= C\zeta_1^{(m)} + C_1k_mr^{k_m-1} - C_2k_mr^{-k_m-1} \\
\tau_{\theta z}^{(m)} &= -C\left(\frac{\alpha_{34}^{(m)}}{\beta_{44}^{(m)}} - \zeta_1^{(m)}g_1^{(m)}\right) \qquad (14) \\
&- C_1g_k^{(m)}r^{k_m-1} - C_2g_{-k}^{(m)}r^{-k_m-1}
\end{aligned}$$

By satisfying the boundary conditions (10) and (11) the constants C_1 and C_2 can be expressed in terms of the constant C. By introducing the notations

$$c_m = \frac{a_{m-1}}{a_m};\quad \rho_m = \frac{r}{a_m}\qquad (c_m < 1,\ c_m \le \rho_m \le 1) \qquad (15)$$

the final expressions for the stresses can be written as

$$\begin{aligned}
\sigma_r^{(m)} &= \frac{p_{m-1}c_m^{k+1} - p_m}{1-c_m^{2k_m}}\rho_m^{k_m-1} \\
&+ \frac{p_mc_m^{k_m-1} - p_{m-1}}{1-c_m^{2k_m}}c_m^{k_m+1}\rho_m^{-k_m-1} + C\zeta_1^{(m)}W_1^{(m)} \\
\sigma_\theta^{(m)} &= \frac{p_{m-1}c_m^{k_m+1} - p_m}{1-c_m^{2k_m}}k_m\rho_m^{k_m-1} \qquad (16) \\
&- \frac{p_mc_m^{k_m-1} - p_{m-1}}{1-c_m^{2k_m}}k_mc_m^{k_m+1}\rho_m^{-k_m-1} \\
&+ C\zeta_1^{(m)}W_2^{(m)} \\
\tau_{\theta z}^{(m)} &= -\frac{p_{m-1}c_m^{k_m+1} - p_m}{1-c_m^{2k_m}}g_k^{(m)}\rho_m^{k_m-1} \\
&- \frac{p_mc_m^{k_m-1} - p_{m-1}}{1-c_m^{2k_m}}g_{-k}^{(m)}c_m^{k_m+1}\rho_m^{-k_m-1} + CW_3^{(m)}
\end{aligned}$$

where

$$\begin{aligned}
W_1^{(m)} &= 1 - \frac{1-c_m^{k_m+1}}{1-c_m^{2k^{(m)}}}\rho_m^{k_m-1} \\
&- \frac{1-c_m^{k_m-1}}{1-c^{2k_m}}c_m^{k_m+1}\rho_m^{-k_m-1} \\
W_2^{(m)} &= 1 - \frac{1-c_m^{k_m+1}}{1-c_m^{2k_m}}k_m\rho_m^{k_m-1} \\
&+ \frac{1-c_m^{k_m-1}}{1-c_m^{2k_m}}k_mc_m^{k_m+1}\rho_m^{-k_m-1} \\
W_3^{(m)} &= -\zeta_2^{(m)} + \zeta_1^{(m)}\left(\frac{1-c_m^{k_m+1}}{1-c_m^{2k_m}}g_k^{(m)}\rho_m^{k_m-1}\right. \\
&+ \left.\frac{1-c_m^{k_m-1}}{1-c_m^{2k_m}}g_{-k}^{(m)}c_m^{k_m+1}\rho_m^{-k_m-1}\right)
\end{aligned}$$

$$\zeta_2^{(m)} = \frac{(\alpha_{13}^{(m)}-\alpha_{23}^{(m)})(\beta_{14}^{(m)}+\beta_{24}^{(m)})-\alpha_{34}^{(m)}(\beta_{11}^{(m)}-\beta_{22}^{(m)})}{\beta_{22}^{(m)}\beta_{44}^{(m)}-\beta_{24}^{(m)2}-(\beta_{11}^{(m)}\beta_{44}^{(m)}-\beta_{14}^{(m)2})}$$

In equation (16) p_{m-1} and p_m denote the normal forces acting on internal and external surfaces of the *m-th* layer. The remaining unknown forces and constant C are determined from the boundary conditions (11) and (12). These expressions are rather complicated and will be derived in the next section.

By the above, we have adapted the solution obtained by Lekhnitskii in [4] for a multilayered closed–ended cylinders.

2.3 Evaluation of Interface Forces and Constant of Integration

Next we shall derive the system of equations which will be used later for the calculation of the unknown interface forces $p_1,\ p_2,\ldots,p_{nl-1}$ and the constant of integration C. The first $nl-1$ equations of the system of equations are derived by satisfying the displacement continuity conditions at the interfaces, i.e.

$$\varepsilon_\theta^{(m)} = \varepsilon_\theta^{(m+1)} \qquad \text{at } r = a_m \qquad (17)$$

which gives us the following system of $nl-1$ equations

$$\varepsilon_\theta^{(m)} - \varepsilon_\theta^{(m+1)} = 0 \qquad m = 1,2,\ldots,nl-1 \quad (18)$$

ISBN: 978-1-61804-146-3

for p_m, where

$$\varepsilon_\theta^{(m)} = \alpha_{12}^{(m)}\sigma_r^{(m)} + \alpha_{22}^{(m)}\sigma_\theta^{(m)} + \alpha_{23}^{(m)}\sigma_z^{(m)} + \alpha_{24}^{(m)}\tau_{\theta z}^{(m)} \quad (19)$$

By substituting the stress expressions (16) into the equations for the boundary conditions (18), and after rearranging terms and simplification, we arrive at the set of equations for unknown forces and the constant of integration C:

$$\begin{aligned} & C(\Delta_1^{(m)} - \Delta_1^{(m+1)}) + p_{m-1}\Delta_2^{(m)} \\ + \quad & p_m(\Delta_3^{(m)} - \Delta_2^{(m+1)}) + p_{m+1}\Delta_3^{(m+1)} = 0 \end{aligned} \quad (20)$$

where

$$\begin{aligned} \Delta_1^{(m)} &= \alpha_{23}^{(m)} + \zeta_1^{(m)}(W_1^{(m)}\beta_{12}^{(m)} + W_2^{(m)}\beta_{22}^{(m)}) \\ &+ W_3^{(m)}\beta_{24}^{(m)} \\ \Delta_2^{(m)} &= \frac{f_1^{(m)}f_3^{(m)} - f_4^{(m)}}{f_9}\beta_{12}^{(m)} \\ &+ \frac{f_1^{(m)}f_5^{(m)} + f_6^{(m)}}{f_9}\beta_{22}^{(m)} \\ &- \frac{f_1^{(m)} + f_7^{(m)} - f_8^{(m)}}{f_9}\beta_{24}^{(m)} \\ \Delta_3^{(m)} &= \frac{f_2^{(m)}f_4^{(m)} - f_3^{(m)}}{f_9}\beta_{12}^{(m)} \\ &- \frac{f_2^{(m)}f_6^{(m)} + f_5^{(m)}}{f_9}\beta_{22}^{(m)} \\ &- \frac{f_2^{(m)}f_8^{(m)} - f_7^{(m)}}{f_9}\beta_{24}^{(m)} \\ & m = 1, \ldots, nl-1 \end{aligned}$$

Where the coefficients $f_i^{(m)}$, $i = 1, 2, \ldots, 9$ are the functions which depend on geometrical and physical properties [6]. It is apparent that when we consider a couple of adjacent layers, we do all the calculations at the top of the layer m and at the bottom of the layer $m+1$ with the same radius a_m.

The total number of unknown terms in the system of equations (20) is equal to the number of the layers nl, whereas the number of equations is $nl-1$. Therefore, in order to solve this system we need one more equation, namely the equation (12) which contains the piecewise integral. After the integration the additional equation can be written in the following form

$$\begin{aligned} & \sum_{m=1}^{nl} \left(p_{m-1}\lambda_1^{(m)} + p_m\lambda_2^{(m)} + C\lambda_3^{(m)} \right) \\ = \quad & \pi(p_0 - p_{nl})a_0^2 + F \end{aligned} \quad (21)$$

Unlike the system (20), the expression (21) represents only a single equation calculated as a sum through the thickness, with m varying from 1 to nl. The expressions for the coefficients λ_1, λ_2 and λ_3 are rather cumbersome and can be found in [6].

Finally, it should be noted that when the winding angle $\varphi_m = 0^\circ$ or 90° then we are dealing with an orthotropic layer with cylindrical anisotropy, which means that there are two planes of elastic symmetry, radial and tangential. Then $\alpha_{34}^{(m)} = \beta_{14}^{(m)} = \beta_{24}^{(m)} = g_k^{(m)} = g_{-k}^{(m)} = 0$ and tangential stresses $\tau_{\theta z}^{(m)}$ vanishes. In the case when $\varphi_m = 0^\circ$

$$k_m = \sqrt{\frac{\beta_{11}^{(m)}}{\beta_{22}^{(m)}}} = 1 \quad (22)$$

and some denominators containing k_m become equal to zero that leads to singularity. In actual computation, this difficulty can be overcome by assigning a very small number for φ_m (e.g. $= 0.001^\circ$) when $\varphi = 0^\circ$.

3 Failure Criterion and Optimization Method

The strength of filamentary composites is determined by the tensile and compressive strengths in the fibre directions and by the shear strength of the composite material. In composite structures, tensile, compressive and shear stresses may result even from simple loading conditions, and therefore the failure mode of composite structures is rather complicated. Thus, an appropriate failure criterion must be used for the analysis of such structures. In the case of the composite pressure vessels the problem is simplified by the fact that there are no compressive stresses present.

The Tsai–Hill failure criterion is well suited here; it takes into account only the tensile and shear strengths. It considers the distortion portion of the strain energy which causes the shape change. The assumption of the Tsai–Hill criterion is that there exists a failure surface in the stress space and, in the case of laminated pressure vessels possessing cylindrical anisotropy, for the m-th layer can be expressed in the following form:

$$\frac{\sigma_1^{(m)2}}{X_t^{(m)2}} - \frac{\sigma_1^{(m)}\sigma_2^{(m)}}{X_t^{(m)2}} + \frac{\sigma_2^{(m)2}}{Y_t^{(m)2}} + \frac{\tau_{12}^{(m)2}}{S^{(m)2}} = 1 \quad (23)$$

where X_t and Y_t are longitudinal and transverse tensile strengths,respectively, and S is the shear strength. The above equation is then used to calculate the critical pressure P_{cr} at any point through the thickness. It should be noted that the normal stresses σ_1, σ_2 and shear stress τ_{12} are stresses computed in the material coordinates.

The design objective is the maximization of the burst pressure P_{cr} subject to the failure criterion (23). The design problem for a multilayered pressure vessel of a given thickness ratio a_{nl}/a_0 and number of layers nl can be stated as

$$P_{max} \stackrel{\text{def}}{=} \max_{\bar{\varphi}} P_{cr}(\bar{\varphi}, r) = \max_{\bar{\varphi}} \min_{r} P_{cr} \qquad (24)$$

where

$$\bar{\varphi} = \{\varphi_1, \varphi_2, \varphi_3, \ldots, \varphi_{nl}\}^T \qquad (25)$$

Taking into account the cost constraint the final expression can be written as

$$P_{max} = \max_{\bar{\varphi}} \min_{r} P_{cr} - \max\left[0, \xi \cdot V_C\right]^2 \qquad (26)$$

where ξ is the penalty constant used and V_C is the cost violation for the entire package.

The optimization procedure involves the stages of iteratively improving $\varphi_{opt}^{(m)}$, $m = 1, 2, \ldots, nl$ in order to maximize P_{cr} for a given radius, thickness ratio and constraint.

These type of problems are computationally highly complex and require the use of a fast and reliable multi–dimensional optimization method. The Big Bang – Big Crunch (BB-BC) method [2] has quickly demonstrated its superiority over other heuristic population-based search techniques when employed to perform structural optimization tasks, eg. for the optimal design of space trusses [1], skeletal structures [3], for parameter estimation in structural systems [8] as well as a number of other successful applications.

The Big Bang – Big Crunch algorithm is a heuristic population-based evolutionary optimization method. Among the merits of this method are computational simplicity, ability to handle multidimensional problems and very fast convergence.

4 Numerical Results and Conclusions

The method developed is implemented for the design optimization of pressure vessels of two thickness ratios, $a_{nl}/a_0 = 1.01$ and 1.1, and different number of layers. Three different composite materials are used: Carbon/, S-2 Glass/ and Kevlar-49/Epoxy. The cheapest material here is E-Glass, while Carbon is the most expensive. By using relative quantities the cost factor can be expressed as 1.0 for E-Glass, 6.25 for Carbon, and 4.375 for Kevlar-49, while the densities are $1900 kg/m^3$, $1500 kg/m^3$ and $1300 kg/m^3$, respectively. The material data are taken from ISO 12215 which are the recommended values of the International Organization for Standardization.

The simplest case of optimization is a single-layered cylinder where there is only one design variable φ. It is well established fact that for the single-layered cylinder, depending on its thickness ratio and material properties, the optimal fiber orientation φ_{opt} is in range of $54-57°$; see for example [5]. This fact is illustrated for three different materials in Fig. 1. This

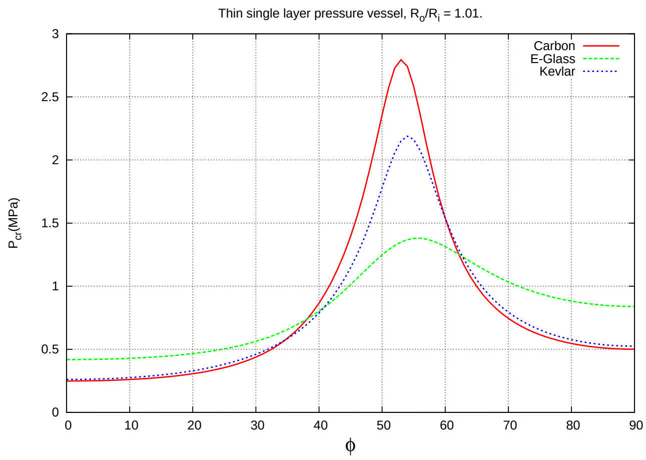

Figure 1: Critical pressure in a thin single layered pressure vessel vs the fiber orientation calculated for different composite materials.

figure clearly demonstrates how the performance of the structure depends on the fiber orientation (φ). It also can be seen that both the Carbon and Kevlar are much more sensitive to the change in angle φ. The above fact is further supported by Fig. 2, which shows a graphical representation of the functional space of the three-dimensional optimization problem for a thin $(a_{nl}/a_0 = 1.01)$ two-layered cylinder. Clearly, the complexity of the functional space will increase even more with the increase in dimensionality, yet it offers us unmatched possibilities for the optimization.

As an example of the maximization of the burst pressure subjected to the cost constraint we consider thin and thick ten-layered pressure vessels. The results of the optimization are shown in the next two figures, Fig. 3 and Fig. 4. Since the weight factor is not used during the optimization procedure, it is calculated later to show its impact on the structure. An important characteristic derived from these graphs is the ratio of the relative bust pressure to the cost factor. For example, in the case of the thin cylinder and the cost constraint set to 40%, we have 37.5% of the cost reduction, while the burst pressure calculated is reduced to only 61.5%. In this case we have six layers made

ISBN: 978-1-61804-146-3

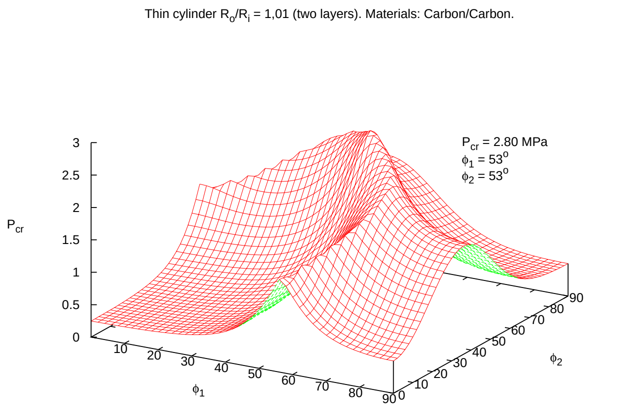

Figure 2: Critical pressure plotted against ply angles for a thin two-layered pressure vessel.

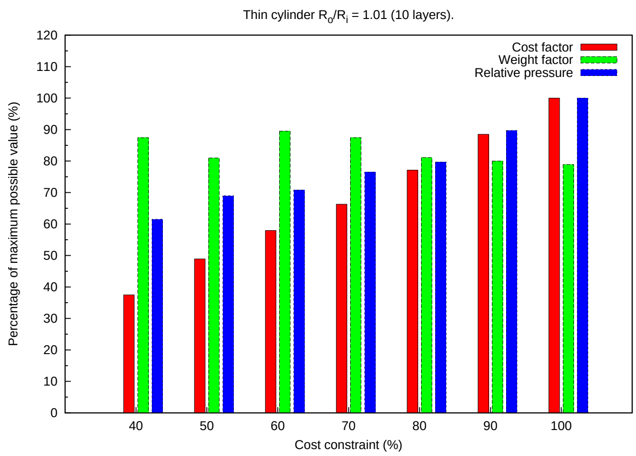

Figure 3: The optimal burst pressure compared to the cost and weight factor subject to the cost constraint and the choice of three materials in the thin pressure vessel.

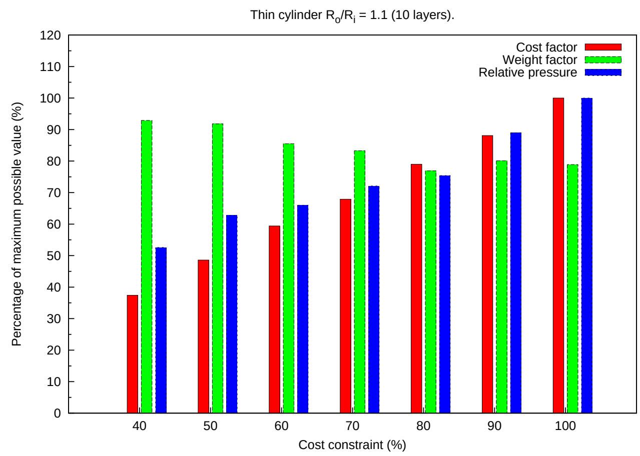

Figure 4: The optimal burst pressure compared to the cost and weight factor subject to the cost constraint and the choice of three materials in the thick pressure vessel.

of E-Glass and four layers of Kevlar-49. This result is achieved with the fiber orientation $43°/43°/42°/42°$ and the rest of layers 69° each. As it can be seen from the graphs, in most cases, this ratio is in favour of the critical pressure. The detailed results for each type of the optimization problem are not given here due to limited space.

References:

[1] C.V. Camp, Design of Space Trusses using Big Bang – Big Crunch Optimization, *J. of Struct. Eng.* 133(7), 2007, pp. 999-1008.

[2] O.K. Erol and I. Eskin, New Optimization Method: Big Bang–Big Crunch, *Advances in Eng. Soft.* 37, 2006, pp. 106–111.

[3] A. Kaveh and S. Talatahari, A Discrete Big Bang – Big Crunch Algorithm for Optimal Design of Skeletal Structures, *Asian J. of Civil Eng. (Building and Housing)* 11(1), 2010, pp. 103-122.

[4] S.G. Lekhnitskii, *Theory of Elasticity of an Anisotropic Elastic Body*, Transl. by P. Fern, Holden-Day, Inc., San Francisco, 1963.

[5] A.K. Roy and S.W. Tsai, Design of Thick Composite Cylinders, *J. of Pressure Techn.* 110(3), 1988, pp.255–263.

[6] P.Y. Tabakov and E.B. Summers, Lay-up Optimization of Multilayered Anisotropic Cylinders based on 3-D Elasticity Solution, *Comp. & Struct.* 84, 2006, pp.374–384.

[7] P.Y. Tabakov, Big Bang – Big Crunch Optimization Method in Optimum Design of Complex Composite Laminates, *World Academy of Science, Eng. and Techn.* 77, 2011.

[8] H. Tang, J. Zhou, S. Xue and L. Xie, Big Bang – Big Crunch Optimization for Parameter Estimation in Structural Systems, *Mech. Syst. and Signal Processing*, 24, 2010, pp. 2888-2897.

[9] M. Walker, T. Reiss and S. Adali, A Procedure to Select the best Material Combinations and Optimally Design Hybrid Composite Plates for Minimum Weight and Cost, *Eng. Opt.* 29, 1997, pp. 65–83.

[10] M. Walker, R. Smith, A procedure to Select the best Material Combinations and Optimally Design Composite Sandwich Cylindrical Shells for Minimum Mass, *Mater. & Design* 27, 2006, pp. 160–165.

ISBN: 978-1-61804-146-3